Title

A testing platform for durability studies of polymers and fiber-reinforced polymer composites under concurrent hygrothermo-mechanical stimuli.

Authors

Gomez, Antonio
Pires, Robert
Yambao, Alyssa
et al.

Publication Date

2014

DOI

10.3791/52464

Peer reviewed

Video Article

A Testing Platform for Durability Studies of Polymers and Fiber-reinforced Polymer Composites under Concurrent Hygrothermo-mechanical Stimuli

Antonio Gomez[1], Robert Pires[1], Alyssa Yambao[1], Valeria La Saponara[1]

[1]Department of Mechanical and Aerospace Engineering, University of California, Davis

Correspondence to: Valeria La Saponara at vlasaponara@ucdavis.edu

URL: http://www.jove.com/video/52464
DOI: doi:10.3791/52464

Keywords: Physics, Issue 94, Fiber-reinforced polymer composites, polymers, hygrothermal, durability, bending, creep

Date Published: 12/11/2014

Citation: Gomez, A., Pires, R., Yambao, A., La Saponara, V. A Testing Platform for Durability Studies of Polymers and Fiber-reinforced Polymer Composites under Concurrent Hygrothermo-mechanical Stimuli. *J. Vis. Exp.* (94), e52464, doi:10.3791/52464 (2014).

Abstract

The durability of polymers and fiber-reinforced polymer composites under service condition is a critical aspect to be addressed for their robust designs and condition-based maintenance. These materials are adopted in a wide range of engineering applications, from aircraft and ship structures, to bridges, wind turbine blades, biomaterials and biomedical implants. Polymers are viscoelastic materials, and their response may be highly nonlinear and thus make it challenging to predict and monitor their in-service performance. The laboratory-scale testing platform presented herein assists the investigation of the influence of concurrent mechanical loadings and environmental conditions on these materials. The platform was designed to be low-cost and user-friendly. Its chemically resistant materials make the platform adaptable to studies of chemical degradation due to in-service exposure to fluids. An example of experiment was conducted at RT on closed-cell polyurethane foam samples loaded with a weight corresponding to ~50% of their ultimate static and dry load. Results show that the testing apparatus is appropriate for these studies. Results also highlight the larger vulnerability of the polymer under concurrent loading, based on the higher mid-point displacements and lower residual failure loads. Recommendations are made for additional improvements to the testing apparatus.

Video Link

The video component of this article can be found at http://www.jove.com/video/52464/

Introduction

Polymer and fiber-reinforced polymer (FRP) composites have been adopted in a variety of engineering structures, ranging from aircraft and spacecraft, naval vessels, civil infrastructure, (see for examples reviews of Katnam *et al.*[1], Hollaway[2], Mouritz *et al.*[3]), cars and trains, wind turbine blades, to prosthetics and biomaterials for sutures and implants. These materials' durability is affected by complex service scenarios, which may include a combination of a) thermo-mechanical loading, *e.g.*, freeze-thaw cycles in civil infrastructure[4], subsonic/supersonic flight profiles[5], wear in metal-backed polyethylene[6]); b) degradation due to environmental and chemical agents, *e.g.*, sea water, de-icing, hydraulic fluid for aerospace and naval structures[7-10], degradation of polymethylmethacrylate dental composites due to saliva[11]; c) complex interactions of materials in fastened or bonded joints, *e.g.*, galvanic corrosion and debonding between dissimilar materials, whether in a carbon/fiber patch repair on an aircraft aluminum skin, or a carbon/PEEK bone plate fastened by stainless steel[12].

There is unfortunately limited knowledge of the impact of concurrent in-service stimuli on the long-term durability of these materials. Most polymers may be categorized as viscoelastic materials. Mechanical loadings and environmental conditions significantly influence the viscoelastic response of polymers. Hence, reliable models for these materials' long-term behavior should be able to incorporate time-dependent responses to coupled hygrothermal, mechanical, chemical stimuli. This in turn will improve design predictions, safety and condition-based maintenance/ replacement protocols.

There is a large literature body on experimental testing on hygrothermal effects, for example hygrothermal diffusion tests: if the scale of the samples allows it, the material samples may be positioned in a chamber at desired humidity and temperature levels. The samples are removed periodically to measure their mass and/or volume changes for a given amount of time, from weeks to years[10,13-17]. The hygrothermal test may be followed by mechanical testing, *i.e.*, residual static/fatigue strength/fracture mechanics testing[17-19], which only gives information on the effect of hygrothermal stimulus on the mechanical responses of materials. Test data may be fitted to diffusion models of varying complexity, from simple Fickian diffusion to models that include dependency on concentration, stress, temperature, reversible physical aging/plasticization and irreversible chemical reactions. This experimental output may be further incorporated in structural analyses.

Few authors have addressed the impact of simultaneous hygrothermal and mechanical stimuli. Among those researching FRP composites, Neumann and Garom[20] immersed stressed and unstressed specimens in distilled water. Stress was applied by positioning the specimens inside compressed stainless steel springs, tuning the load by using different spring stiffnesses and compressive loads. A similar procedure is reported by Wan *et al.*[21]. Helbling and Karbhari[22] employed a bending fixture inside an environmental chamber for different relative humidity percentages (RH%) and temperature levels. The pre-conditioned specimens were subjected to a given bending strain level, corresponding to a percentage of the static ultimate tensile strain for that composite. Kasturiarachchi and Pritchard[23] prepared a stainless steel 4-point bending

jig (one per specimen) that was positioned on a shelf in a large glass desiccator. The desiccator was partially filled with distilled water, had small leaks to prevent the buildup of pressure, and was placed in a humidity chamber at 95% RH. Gellert and Turley[7] investigated marine-grade FRP composite specimens for their durability under combined creep loading and 100% RH. Their samples were loaded in 4-point bending at a constant load equal to 20% of the failure static flexure load, while fully immersed in sea water. The creep deflection was acquired periodically by using a thickness gauge between the outer surface of the beam in the central cross-section, and a glass plate (it is inferred that such measurement was performed outside the chamber). Abdel-Magid *et al.*[24] placed samples of glass/epoxy in an Invar environmental fixture which was provided by NASA Langley, as the specimens were loaded in tension along the fiber direction, at 20% of the ultimate axial load. Ellyin and Rohrbarcher[25] ran hygrothermal tests for up to 140 days, and then tested the specimens in fatigue on a hydraulic testing machine. The specimens were wrapped in a wet cheese cloth connected to a tube and a water supply. Earl *et al.*[26] positioned their loading fixture and the specimens in a large environmental chamber (5.5 m^3).

As discussed in many experimental studies, the environmental conditions affect the polymers' mechanical properties and responses. Some limited experiments also show that the existence of mechanical stress/strain influences the diffusion process in the polymers. Hence, to enhance understanding on the overall performance of polymer-based materials under both mechanical and non-mechanical effects, there is a need for concurrent testing.

There were several objectives behind the design of the testing platform discussed in this paper. First, the platform is part of the experimental setup in a multi-year investigation on the hygrothermo-mechanical behavior of different types of FRP sandwich composites for wind turbine and naval engineering applications. The test data are used to calibrate the parameters in the viscoelastic constitutive equations for the polymeric composites. The constitutive models are based on the work developed over the years by Muliana and collaborators[27-30]. The second objective was to have a low-cost and user-friendly testing platform, for example one that could be easily relocated in a laboratory (*e.g.*, to a scale for mass measurements, or to the source of the fluid, *e.g.*, one coming from a faucet, a fumehood or a flammable cabinet). The third goal was to create a testing platform that is resistant to a number of chemicals commonly used in service (particularly hydraulic fluid, de-icing, cleaning solvents for aerospace applications[8-10]), thus specimens could be immersed in such chemicals, and their durability could be assessed.

The chamber (**Figure 1**) was constructed with high-density polyethylene, which has high chemical resistance. As mentioned above, it is expected that future work will include hygrothermo-mechanical investigation of composites immersed in hydraulic fluid, de-icing, cleaning solvents. Since thermal regulation is an integral aspect of testing, expanded polystyrene foam was fit around the sides of the tank and secured in place by tape and the steel frame itself, to prevent heat exchange with the environment.

The lid of the chamber (**Figure 2**) was manufactured from transparent, 9.525 mm-thick polycarbonate, allowing the users to observe the specimens during testing without disturbing the test. The lid is secured in place by aluminum T-bars, which were machined to slide under overhanging brackets on the sides of the tank.

Bending in the specimens is enacted by three aluminum blocks, which hang down from the lid, and are fastened through slots in the lid. The three blocks allow up to four specimens to be tested at one time, while the lid slots allow the block spacing to be adjusted depending on the length of the specimens. Each block is rounded at the contact edge to a 12.7 mm diameter, in adherence to ASTM standard D790-10. The specimens are positioned beneath two of the three blocks, with an upward force applied at its center to induce bending (**Figures 1-2**).

The apparatus was designed with maximum versatility and ease-of-use in mind. Casters with 41.275 mm diameter are fastened beneath the chamber for mobility purposes. Above them, the tank is supported by a welded steel frame with a wire mesh bottom and cross beams for support. Angle stock spacers for the outside tank corners were manufactured to keep the insulation from being crushed by the overhead weight and displacement gauges (string pot apparatus, discussed later). Around the top, angle stock was used again for framing. Pulley and string potentiometer systems to measure mid-span deflection are mounted on four steel, square-tubing arches (**Figure 3**). The center two arches out of these four carry the string potentiometers and are adjustable to account for specimen versatility. The string potentiometers were constructed using a torsional spring (as can be found in retractable key lanyards) and potentiometers with three-pronged electronic outputs. The pulleys are aligned and mounted for use with a steel cable running from a rigid connection by the specimen to a hanging rod over the side of the chamber for adjustable weight application.

The load is applied to the specimen using a series of cables, pulleys, linkages and bolts. First, the specimen is placed into the U-bolt so that the 10 mm cross bar is contacting the middle of the span. A 9.525 mm diameter steel rod with eye bolts at each end is then connected to the U-bolt. This steel connection passes through the lid of the chamber. A steel cable and Kevlar thread are attached to the eyebolt opposite the U-bolt. This allows the Kevlar thread from the string potentiometer to read data from a rigid point. The steel cable continues upwards and passes over two pulleys that allow the load to be applied at the periphery of the tank. The cable is then attached to a 9.525 mm diameter steel rod that serves as a slotted weight hanger. This hanger provides a place where the slotted weights can be set in order to apply the desired load.

Protocol

1. Loading the Specimens

1. Raise the lid of the tank and rest it upon the side supports (**Figure 4**).
2. Place the specimen in the U-bolt, and ensure that the cross bar is making contact at the center of the specimen.
3. Rest the ends of the specimen on the aluminum supports hanging from the lid. The ends of the specimens should have 5-10 mm of overhang.
4. Repeat steps 1.2-1.4 for all of the specimens that will be tested.
5. Remove the lid supports, lower lid, and make sure that the lid is seated on the lip of the tank.
6. Apply the desired force by adding weights to the steel rod next to the outer pulley.

2. Measuring Displacement

1. Ensure that the string potentiometer line is pulled taut.
2. Using a digital multimeter, measure the resistance across the outer pins of the potentiometer (**Figure 3**), with black to Pin 1 and red to Pin 3, and record the reading.
3. Convert the resistance reading into a displacement reading by computing the calibration factor (in this case, 1 kΩ corresponds to a 64.895 mm displacement).
4. Repeat steps 2.1-2.3 for each specimen.

3. Weighing the Specimens

1. Before beginning the weighing procedure, record the displacement data and prepare an interim holding chamber filled with the testing fluid at RT, as per ASTM D5229[31], or the appropriate testing standard.
2. Remove the slotted weights from the ends of the steel cables.
3. Raise the lid of the tank and rest it upon the side supports.
4. Remove the specimen and place it into the prepared interim holding chamber. Repeat this step for all of the specimens.
5. Remove the specimens and dry them individually using a microfiber cloth in order to remove excess fluid.
6. Place the specimen on a high-precision scale and record the data reading.
7. Repeat steps 3.5-3.6 for all specimens and then follow **Protocol Step 1**.

Representative Results

The testing apparatus has successfully held specimens immersed in a fluid under three-point bending. With reasonable precisions, specimens can be loaded and tested with accurate readouts from the potentiometers for mid-point deflection changes. The change in electrical resistance can be recorded to 4 significant figures, resulting in a displacement resolution of the order of 0.1 μm.

Hygrothermo-mechanical tests were conducted at RT on two groups of four specimens of closed-cell polyurethane foam, with nominal dimensions 215 mm length x 24 mm width x 18 mm thickness. One group was tested in the chamber under dry conditions, intended as a) in air, inside the tank, and b) at ambient relative humidity of ~50% RH (the test took place at the end of June in a laboratory situated in hot and dry northern California Central Valley, in USA). This first group of samples is herein indicated as 'dry specimens'. The second group of samples was tested in the tank while fully immersed in deionized water (100% RH, herein indicated as 'wet specimens'). The specimens were loaded with hanging weights approximately equal to 50% of their ultimate load under static dry conditions, resulting in (1.780 ± 0.116) kg. The application of each hanging weight took few seconds, to achieve quasi-static loading conditions. It was expected that the foam would have a nonlinear viscoelastic behavior, but it was not known a priori how the concurrent stimuli would decrease the foam durability with respect to the dry specimens.

Resistance measurements on the digital multimeter were taken for each specimen, at approximately 15 min intervals for the first 6 hr of testing. Measurements were taken again after an additional 18 hr. From this, the change in mid-span deflection was tracked. Based on the data collected, the displacement after 24 hr for the dry specimens was (2.141 ± 0.371) mm, while the displacement for the wet specimens was significantly higher, and equal to (14.41 ± 3.62) mm (**Figure 5, Table 1)**.

Following each trial run, the specimens were then tested for residual strength by loading them until failure. The wet specimens were found to have a residual failure load equal to (2.970 ± 0.246) kg, as compared to the residual failure load of (3.623 ± 0.0967) kg for the dry specimens, **(Figure 6, Table 2)**. The resolution for the residual failure load measurements was ± 0.194 kg.

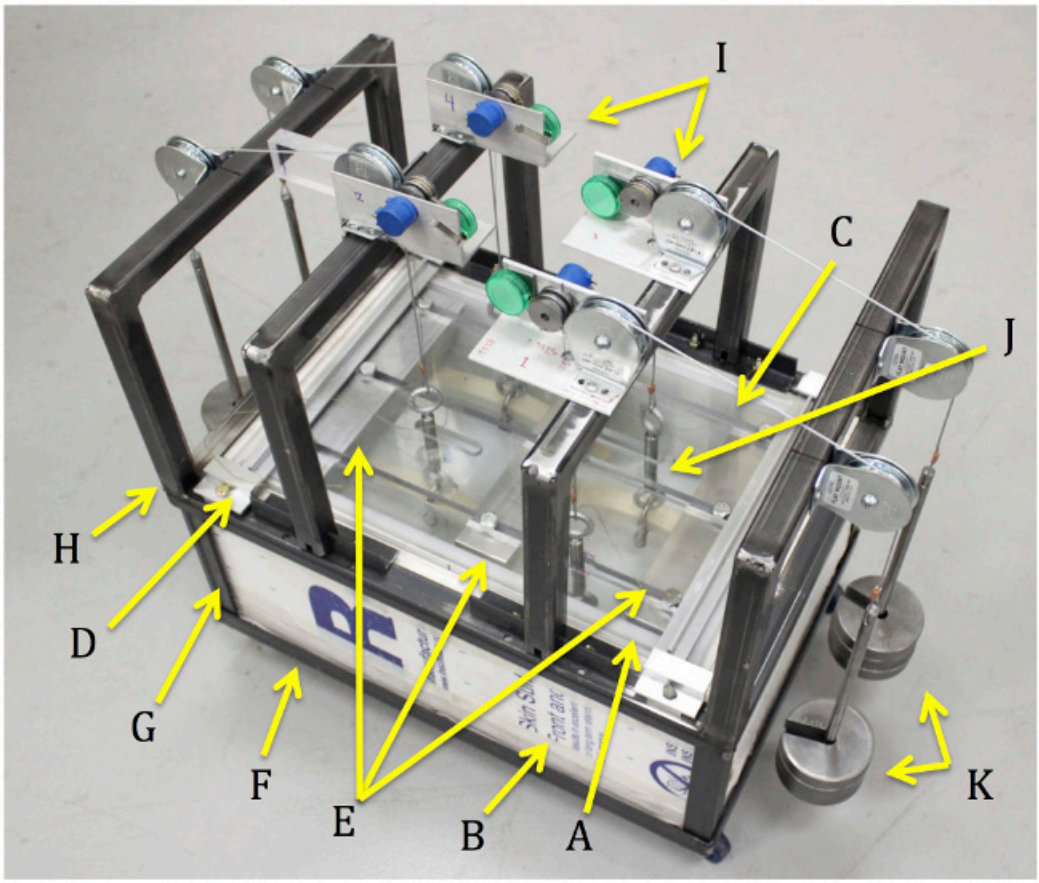

Figure 1. Overview of major components of testing apparatus. A. High density polyethylene tank. B. Expanded polystyrene foam insulation. C. Slotted polycarbonate lid. D. Aluminum T bar and overhang bracket. E. Three-point bending supports. F. Bottom frame. G. Angle spacers. H. Top frame. I. String potentiometer assemblies. J. Lower loading assembly. K. Slotted weights and hanger. Please click here to view a larger version of this figure.

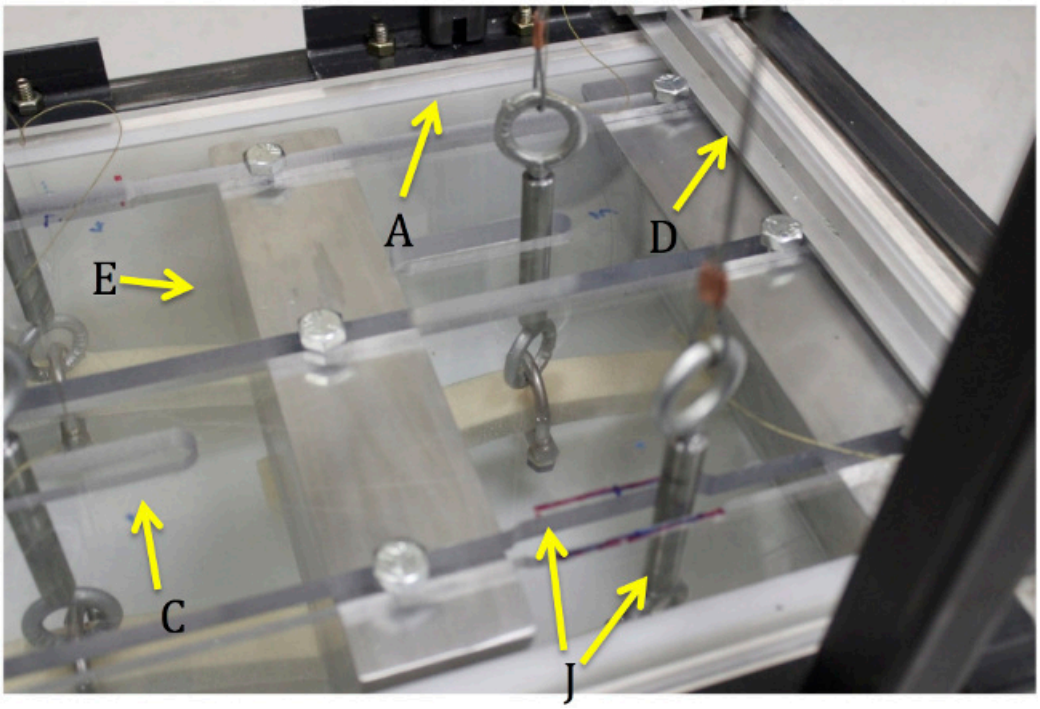

Figure 2. Detailed view of lid. A. High density polyethylene tank. C. Slotted polycarbonate lid. D. Aluminum T-bar and overhang bracket. E. Three-point bending supports. J. Lower loading assembly. Please click here to view a larger version of this figure.

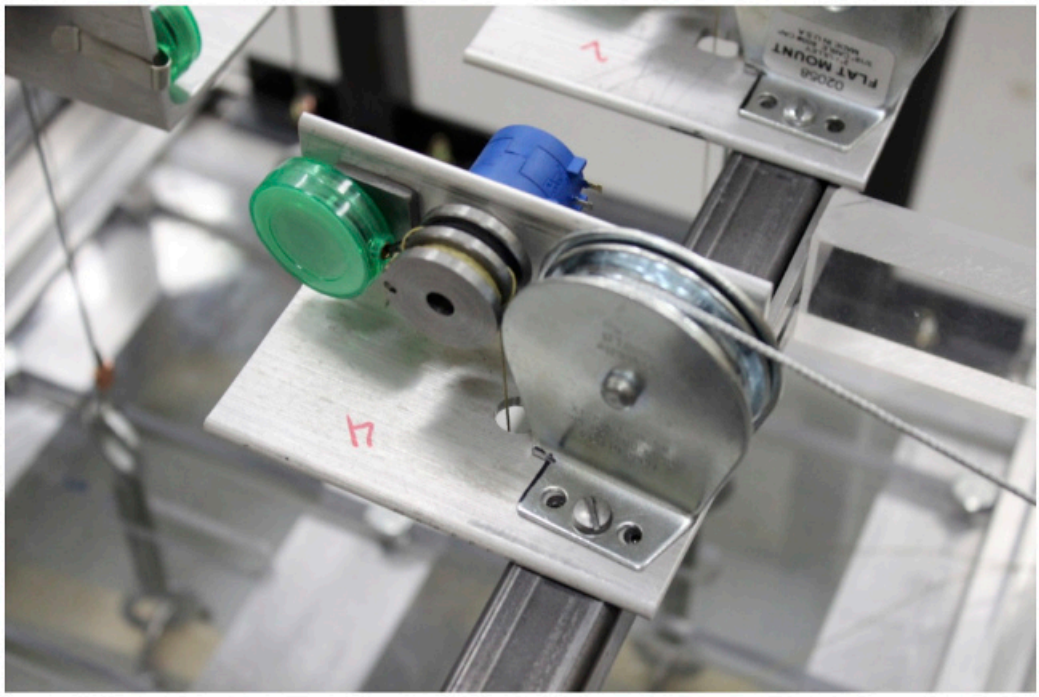

Figure 3. String potentiometer assembly of the testing apparatus. Please click here to view a larger version of this figure.

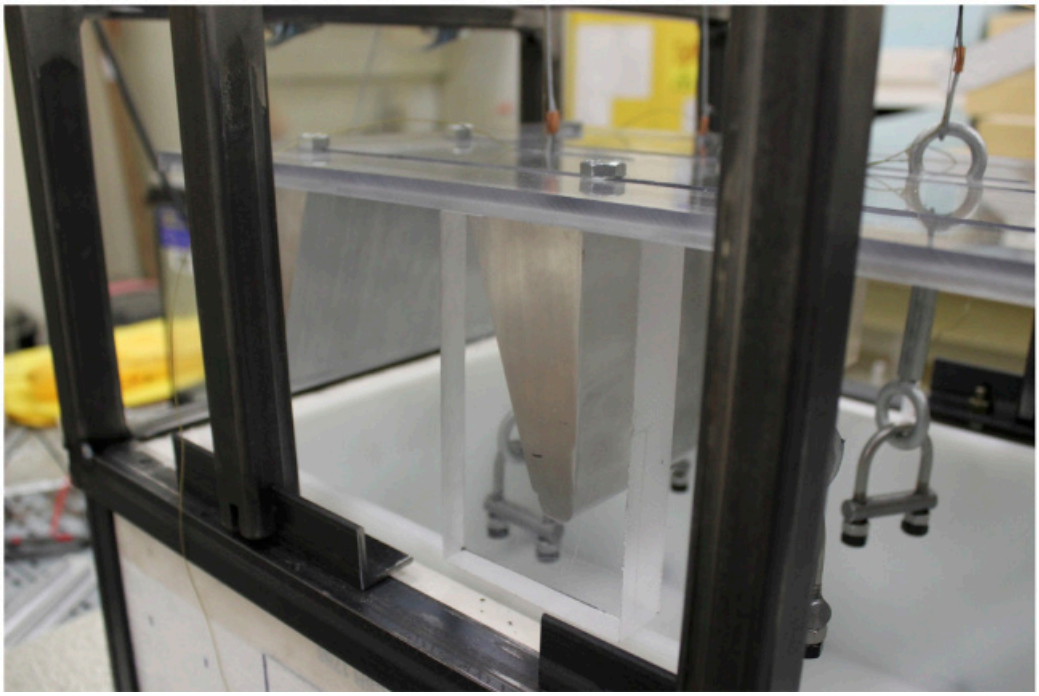

Figure 4. Lid supports of the testing apparatus. Please click here to view a larger version of this figure.

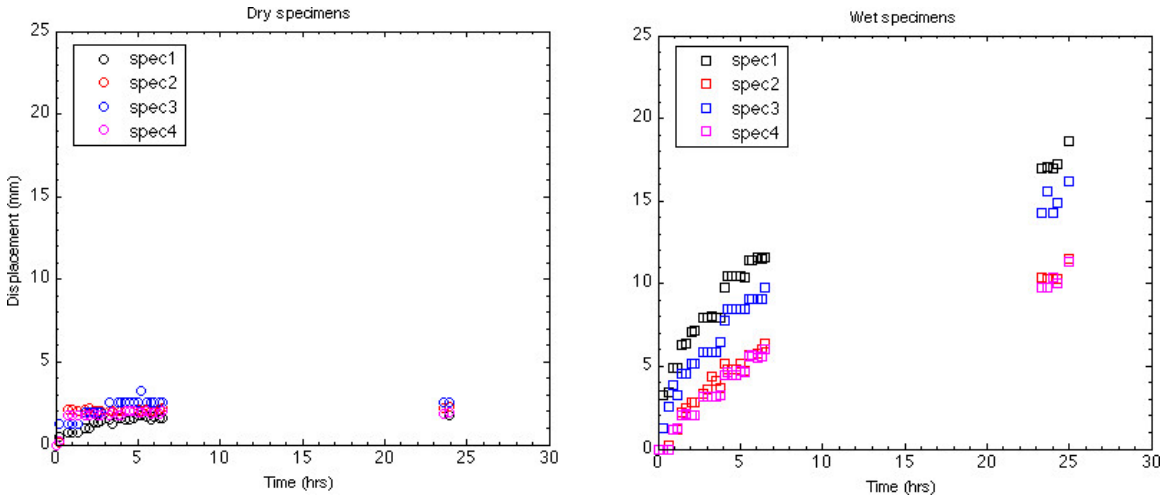

Figure 5. Mid-span displacement variation with time, for dry and wet specimens. Please click here to view a larger version of this figure.

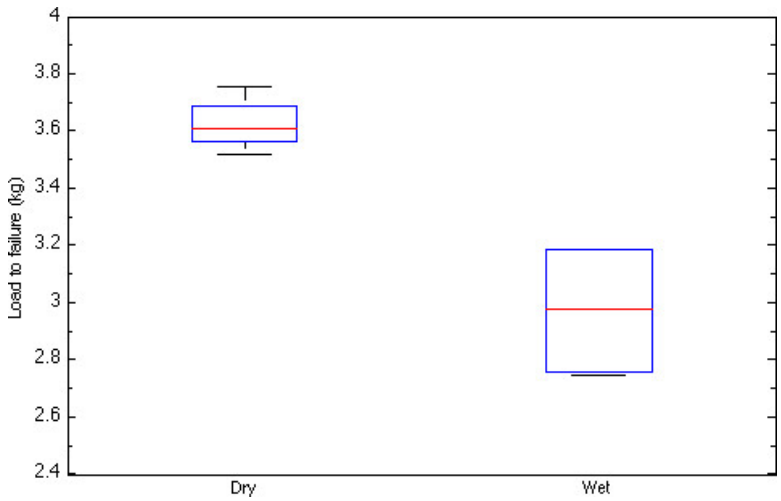

Figure 6. Box plots of residual loads to failure, for dry and wet specimens, showing the larger vulnerability of the wet specimens.
Please click here to view a larger version of this figure.

Figure 7. Pictures of foam specimens after residual bending strength tests: (**A**) and (**B**) dry specimens, (**C**) and (**D**) wet specimens. The nominal specimen width is 24 mm. Please click here to view a larger version of this figure.

Hours from start	Change of displacement (mm), specimen 1	Change of displacement (mm), specimen 2	Change of displacement (mm), specimen 3	Change of displacement (mm), specimen 4
0.000	0.000	0.000	0.000	0.000
0.230	0.454	0.130	1.298	0.195
0.730	0.714	2.141	1.298	1.817
0.980	0.779	2.141	1.298	1.817
1.310	0.779	2.076	1.298	1.817
1.810	1.038	2.141	1.947	1.817
2.010	0.973	2.206	1.947	1.817
2.350	1.363	2.076	1.947	1.882
2.610	1.363	2.076	1.947	1.752
2.730	1.428	2.076	1.947	1.752
3.230	1.557	2.076	2.596	1.817
3.480	1.298	2.076	1.947	1.947
3.810	1.622	2.076	2.596	1.817
4.010	1.622	2.076	2.596	1.817
4.230	1.557	2.076	2.596	2.012
4.480	1.557	2.076	2.596	2.012
4.730	1.622	2.076	2.596	2.012
4.980	1.752	2.141	2.596	1.947
5.230	1.752	2.076	3.244	1.947
5.510	1.687	2.141	2.596	2.012
5.780	1.557	2.076	2.596	1.882
5.980	1.687	2.076	2.596	1.947
6.310	1.622	2.141	2.596	1.882
6.480	1.622	2.206	2.596	2.012
23.550	1.882	2.206	2.596	1.882
23.967	1.752	2.271	2.596	1.947

Table 1. Displacement vs. time of foam specimens at ambient relative humidity (dry specimens).

Hours from start	Change of displacement (mm), specimen 1	Change of displacement (mm), specimen 2	Change of displacement (mm), specimen 3	Change of displacement (mm), specimen 4
0.000	0.000	0.000	0.000	0.000
0.303	3.245	0.000	1.298	0.000
0.653	3.439	0.195	2.596	0.000
0.903	4.932	1.168	3.894	1.168
1.163	4.932	1.168	3.245	1.233
1.433	6.295	2.206	4.543	2.012
1.703	6.360	2.466	4.543	2.142
2.013	7.074	2.855	5.192	2.077
2.253	7.203	2.790	5.192	2.077
2.763	7.917	3.310	5.841	3.180
3.013	7.917	3.634	5.841	3.180
3.283	8.047	4.413	5.841	3.180
3.513	7.917	4.153	5.841	3.180
3.753	7.917	3.699	6.489	3.245
4.013	9.734	5.192	7.787	4.478
4.253	10.448	4.802	8.436	4.608
4.513	10.448	4.802	8.436	4.478
4.783	10.448	4.802	8.436	4.478
5.013	10.448	5.127	8.436	4.737
5.313	10.383	4.737	8.436	4.608
5.513	11.421	5.711	9.085	5.581
5.753	11.421	5.646	9.085	5.711
6.033	11.551	5.776	9.085	5.516
6.333	11.486	6.035	9.085	5.581
6.503	11.551	6.360	9.734	6.035
23.300	16.937	10.383	14.277	9.734
23.650	17.067	10.318	15.575	9.734
23.983	17.002	10.253	14.277	10.383
24.250	17.262	10.253	14.926	9.994
24.983	18.625	11.486	16.224	11.292

Table 2. Displacement vs. time of foam specimens at 100% RH (wet specimens).

Discussion

From the acquired data, it can be seen that the concurrent testing scenario did affect the durability of the closed-cell polyurethane foam specimens. This can be seen by comparing the significantly different displacements (**Figure 5**) and residual loads to failure (**Figure 6**) of dry and wet specimens. **Figure 7** shows pictures of the specimens after the residual strength tests. It should also be observed that, while the displacement of the dry specimens reached steady state within the observation interval of 24 hr, those of the wet specimens did not. Hence, future tests will be conducted for a longer time interval, to either achieve a steady-state behavior of the conditioned specimens or establish that such steady-state may not be possible within a given testing time frame (for example, if the material experiences degradation that leads to failure).

The boxplots of **Figure 6** show that the distribution of residual loads to failure for the wet specimens is statically different and lower with respect to the case for the dry specimens.

A direct comparison of this outcome cannot be made with the literature because of the relatively limited published data and the different materials and load profiles selected by various authors. However, the representative results obtained with this fixture concur with the trend observed of Gellert and Turley[7] about “significantly higher” creep deflections experienced by their glass-fiber reinforced samples.

The testing apparatus may be improved in order to increase its robustness and ease of use. Sliding mounts will be added at the base of the top frame supports to hold the potentiometers in a more secure manner. This will reduce the possibility of movement and, therefore, increase the accuracy of the readings. Moreover, the potentiometers will be connected to small breadboards into three-pin screw terminals. This will also enhance the accuracy of the readings because it will eliminate the need to touch the potentiometer while taking measurements.

Additional improvements are planned to further increase the flexibility of the apparatus. For example, a new lid will be developed in order to create an airtight seal when testing potentially harmful chemicals. This change will likely lead to a modification of **Protocol Step 1**. An immersion heater may also be added in order to allow for testing at elevated temperatures. When testing a saline solution, a magnetic stir bar could be considered in place of an expensive stainless steel immersion heater. This would require a modification to the base of the apparatus for the incorporation of a magnetic source. The resulting testing apparatus will provide a broader picture of how the concurrent testing affects the durability of polymers and polymeric matrix composites under a variety of in-service conditions.

Disclosures

The authors have nothing to disclose.

Acknowledgements

The authors thank Destiny Garcia, Serena Ferraro, Erik Quiroz and Steven Kern (Advanced Composites Research, Engineering and Science laboratory) for their help in designing and manufacturing the test setup. Shawn Malone, Michael Akahori, David Kehlet (Engineering Fabrication Lab) are acknowledged for their suggestions and assistance in the machining process. The support of the National Science Foundation (collaborative grant CMMI-1265691 and its REU supplement) and the Office of Naval Research (N00014-13-1-0604 to A. Muliana, Texas &M University (Principal Investigator), and V. La Saponara, managed by program director Yapa Rajapakse) are gratefully appreciated.

References

1. Katnam, K. B., Da Silva, L. F. M., & Young, T. M. Bonded repair of composite aircraft structures: A review of scientific challenges and opportunities. *Prog Aerosp Sci*. **61**, 26-42 (2013).
2. Hollaway, L. C. A review of the present and future utilization of FRP composites in the civil infrastructure with reference to their important in-service properties. *Constr Build Mater.* **24**, 2419-2445 (2010).
3. Mouritz, A. P., Gellert, E., Burchill, P., & Challis, K. Review of advanced composite structures for naval ships and submarines. *Compos Struct.* **53**, 21-41 (2001).
4. Albanilla, M. A., Li, Y., & Karbhari, V. M. Durability characterization of wet layup graphite/epoxy composites used in external strengthening. *Compos Part B-Eng*. **37**, 200-212 (2006).
5. Jedidi, J., Jacquemin, F., & Vautrin, A. Accelerated hygrothermal cyclical tests for carbon/epoxy laminates. *Compos. Part A –Appl. Sci.* **37**, 636-645 (2006).
6. Jones, L. C., Tsao, A. K., & Topoleski, L. D. T. Orthopedic Implant Retrieval and Failure Analysis. In: *Degradation of Implant Materials.* Noam Eliaz, editor. Springer. 393-447 (2012).
7. Gellert, E. P., & Turley, D. M. Seawater immersion ageing of glass-fibre reinforced polymer laminates for marine applications. *Compos. Part A –Appl. Sci.* **30**, 1259-1265 (1999).
8. Sugita, Y., Winkelmann, C., & La Saponara, V. Environmental and chemical degradation of carbon/epoxy lap joints for aerospace applications, and effects on their mechanical performance. *Compos. Sci. Technol.* **70**, 829-839 (2010).
9. Campbell, R. A., Pickett, B. M., La Saponara, V., & Dierdorf, D. Thermal Characterization and Flammability of Structural Epoxy and Carbon/Epoxy Composite with Environmental and Chemical Degradation. *J. Adhes. Sci. Technol.* **26**, 889-910 (2012).
10. Landry, B., LaPlante, G., & LeBlanc, L. R. Environmental effects on mode II fatigue delamination growth in an aerospace grade carbon/epoxy composite. *Compos. A-Appl. Sci.* **43**, 475-485 (2012).
11. Ferracane, J. L. Hydroscopic and hydrolytic effects in dental polymer networks. *Dent. Mater.* **22**, 211-222 (2006).
12. Mueller, Y., Tognini, R., Mayer, J., & Virtanen, S. Anodized titanium and stainless steel in contact with CFRP: An electrochemical approach considering galvanic corrosion. *J. Biomed. Mater. Res. –A*. **82A**, 936-946 (2007).
13. Bagley, E., & Long, F. A. Two-state Sorption and Desorption of Organic Vapors in Cellulose Acetate. *J. Am. Chem. Soc.* **77**, 2172-2178 (1955).
14. Shen, C.-H., & Springer, G. Moisture Absorption and Desorption of Composite Materials. *J. Compos Mater*. **10**, 2-20 (1976).
15. Zhou, J., & Lucas, J.P. Hygrothermal effects of epoxy resin. Part I: the nature of water in epoxy. *Polymer*. **40**, 5505-5512 (1999).
16. Abot, J. L., Yasmin, A., & Daniel I.M. Hygroscopic Behavior of Woven Carbon-Epoxy Composites. *J. Reinf. Plast. Comp*. **24**, 195-207 (2005).
17. LaPlante, G., Ouriadov, A.V., Lee-Sullivan, P., Balcom, B.J. Anomalous Moisture Diffusion in an Epoxy Adhesive. *J. Appl. Polym. Sci*. **109**, 1350-1359 (2008).
18. Weitsman, Y. J. Anomalous fluid sorption in polymeric composites and its relation to fluid-induced damage. *Compos. Part A –Appl. Sci.* **37**, 617-623 (2006).
19. Karbhari, V.M., & Ghosh, K. Comparative durability evaluation of ambient temperature cured externally CFRP and GFRP composiste systems for repair of bridges. *Compos. Part A –Appl. Sci.* **40**, 1353-1363 (2009).
20. Neumann, S., & Marom, G. Free-volume dependent moisture diffusion under stress in composite materials. *J. Mater. Sci.* **21**, 26-30 (1986).
21. Wan, Y.Z., Wang, Y.L., Huang, Y., He, B.M., & Han, K.Y. Hygrothermal aging behaviour of VARTMed three-dimensional braided carbon-epoxy composites under external stresses. *Compos. Part A –Appl. Sci.* **36**, 1102-1109 (2005).
22. Helbling, C. S., & Karbhari, V.M. Investigation of the Sorption and Tensile Response of Pultruded E-Glass/Vinylester Composites Subjected to Hygrothermal Exposure and Sustained Strain. *J. Reinf. Plast. Comp.* **27**, 613-638 (2008).
23. Kasturiarachchi, K. A., & Pritchard, G. Water absorption of glass/epoxy laminates under bending stresses. *Composites*. **14**, 244-250 (1983).

24. Abdel-Magid, B., Ziaee, S., Gass, K., & Schneider, M. The combined effects of load, moisture and temperature on the properties of E-glass/epoxy composites. *Compos Struct.* **71**, 320-326 (2005).
25. Ellyin, F., & Rohrbarcher, C. The Influence of Aqueous Environment, Temperature and Cyclic Loading on Glass-Fibre/Epoxy Composite Laminates. *J Reinf Plast Comp*. **22**, 615-636 (2003).
26. Earl, J. S., Dulieu-Barton, J. M., & Shenoi, R. A. Determination of hygrothermal ageing effects in sandwich construction joints using thermoelastic stress analysis. *Compos Sci Technol.* **63**, 211-223 (2003).
27. Jeon, J., Muliana, A., & La Saponara, V. Thermal stress and deformation analyses in fiber reinforced polymer composites undergoing heat conduction and mechanical loading. *Compos. Struct.* **111**, 31-44 (2014).
28. Muliana, A. H., Rajagopal, K. R., & Wineman. A. A new class of quasi-linear models for describing the non-linear viscoelastic response of materials. *Acta Mech*. **224**, 2169-2183 (2013).
29. Joshi, N., & Muliana, A., Deformation in Viscoelastic Sandwich Composites Subject to Moisture Diffusion. *Compos. Struct*. **92**, 254-264 (2010).
30. Muliana, A. H., & Sawant, S. Viscoelastic Responses of Polymer Composites with Temperature and Time Dependent Constituents. *Acta Mech*. **204**, 155-173 (2009).
31. Standard Test Method for Moisture Absorption Properties and Equilibrium Conditioning of Polymer Matrix Composite Materials. *ASTM International.* (2004).

